Highly selective vapochromic fluorescence of polycarbonate films doped with an ICT-based solvatochromic probe

Muzaffer Ahmad,[a] Irina Platonova,[b] Antonella Battisti,[c] Pierpaolo Minei,[b] Giuseppe Brancato,[a] Andrea Pucci[b,d]*

[a]Scuola Normale Superiore, Piazza dei Cavalieri 7, I-56126 Pisa, Italy
[b]Dipartimento di Chimica e Chimica Industriale, Università di Pisa, Via G. Moruzzi 13, 56124 Pisa, Italy
[c]NEST – Scuola Normale Superiore, Istituto Nanoscienze – CNR (CNR-NANO), piazza San Silvestro 12, 56127 Pisa Italy
[d]INSTM, UdR Pisa, Via G. Moruzzi 13, 56124 Pisa, Italy
Correspondence to: Andrea Pucci (E-mail: andrea. pucci@unipi.it)
(Additional supporting information may be found in the online version of this article)

ABSTRACT

The vapochromic properties of a fluorescent 3-[2-(4-nitrophenyl) ethenyl]-1-(2-ethylhexyl)-2-methylindole (NPEMI-E) characterized by intramolecular charge transfer (ICT) character, dispersed in polycarbonate (PC) films is reported. NPEMI-E solvatochromism is investigated by means of experimental and computational methods. Fluorescent PC films containing 0.1 wt% of NPEMI-E are prepared and exposed to saturated atmospheres of different volatile organic compounds (VOCs). NPEMI-E/PC films show remarkable and reversible vapochromism when exposed to VOCs with high polarity index and favorable interaction with PC matrix such as $CHCl_3$. Only minor variations of the emission wavelength are actually recorded for all other classes of VOCs investigated. The hue parameter is also used for the effective extraction of spectral information from digital color images without the need for wavelength discriminators. Overall, the present results support the use of NPEMI-E/PC films for the cost-effective detection of $CHCl_3$ vapors.

KEYWORDS: vapochromism, salvatochromism, volatile organic compounds, polymer films

INTRODUCTION

Nowadays, chromogenic fluorescent (fluorogenic) materials are highly desirable since their optical properties in emission are well sensitive to different external stimuli such as viscosity and polarity of the environment.[1–3] This feature has been explored for many classes of fluorogenic polymers triggered by potential applications in the field of chemical optical indicators and polymer sensors.[4–8] The fluorescent properties generally depend on different molecular parameters, such as structural flexibility, electron donor or acceptor moieties in addition to an extended conjugation. For example, certain fluorophores characterized by the flexibility of their structure have attracted outstanding interests in materials science being their emission intensity strongly affected by the viscosity of the environment.[9–14] This feature allowed the preparation of fluorogenic polymer films that can easily detect the presence of well-interacting volatile organic compounds (VOCs) such as chloroform and toluene. In detail, once absorbed by the film, the VOC induces a relaxation of the macromolecular chains, which

is followed by an increase in the free volume and a consequent decrease in the local polymer microviscosity, which, in turn, quenches the film fluorescence.[15–17] Nevertheless, even if the explored vapochromism resulted very promising for applications in thin film as accessible optical indicators, the concomitant responses towards viscosity and polarity variations should be averted in certain applications since they might compromise device sensitivity and selectivity. Selectivity is indeed one of the major issues that optical indicators and colorimetric sensors to VOCs are facing today.[18] Notably, the selective identification of aromatic or chlorinated VOCs is extremely important since they have adverse effects on human health.[19] Inspired by previous results on vapochromism, in the present study we focus attention on the solvatochromic features of the 3-[2-(4-nitrophenyl) ethenyl]-1-(2-ethylhexyl)-2-methylindole (NPEMI-E) (Fig. 1).

< Figure 1 near here >

NPEMI-E has been already studied by our group[20,21] for the preparation of stable indole-derived glass blends having very high photorefractive gain. Notably, the presence of asymmetric 2-ethylhexyl group on the nitrogen atom of indole ring hinders the crystallization and aggregation of the molecule, while the electron-withdrawing nitro group in conjugation with the indole ring serves to promote the intramolecular charge transfer (ICT) behavior upon excitation.

Herein, we reported the excellent solubility of NPEMI-E in many classes of solvents flanked by a pronounced change in color depending on solvent polarity. Conversely, no variation of the emission features was detected by changing the solution viscosity. The photophysical properties of the dye, such as the ICT character of its excited state and the observed batochromic shift in emission, were investigated by means of quantum mechanical calculations. The derived solvatochromic features suggested the incorporation of NPEMI-E in a transparent and amorphous polycarbonate (PC) matrix to investigate their potential vapochromism towards the exposure to volatile organic compounds with different polarities. PC was chosen because of its excellent transmittance of light, high impact strength and thermal stability. Furthermore, PC has a polarity index of 2.9, which can be useful for the selective detection of VOCs with high polarity such as chloroform. This work also proposed a new sensitive and cost-effective image processing tool, which can be effectively applied to all the optical sensors already reported in literature.[15]

EXPERIMENTAL

Materials and Methods

All solvents used were purchased from Sigma-Aldrich (Table 1).

Table 1. Vapor pressure, polarity[22], solubility parameter difference Δδ (PC)[23] and refractive index[22] of the utilized solvents.

Polycarbonate (PC), (SABIC, LEXAN® Mw 220000 g $mole^{-1}$ with 1.5 wt% Si) was used as polymer matrix. 3-[2-(4-nitrophenyl)ethenyl]-1-(2-ethylhexyl)-2-methylindole (NPEMI-E) was available in the research group since it had already been synthesized for the optoelectronic applications.[24] ^{1}H NMR confirmed its chemical structure and purity.

^{1}H-NMR (δ, $CDCl_3$, 400 MHz) 0.87 – 0.99 (m, 6H), 1.24 – 1.49 (m, 8H), 1.83 – 2.07(m, 1H), 2.60 (s, 3H, CH_3 indol.), 4.03 (d, 2H, J = 7.69 Hz), 7.17 (d, 1H, J_{trans} = 16.12 Hz), 7.23 – 7.32 (m, 2H,

indol.), 7.32 – 7.39 (m, 1H, indol.), 7.56 (d, 1H, J_{trans} = 16.11 Hz), 7.64 (d, 2H, benz., J = 8.79 Hz), 7.99 – 8.06 (m, 1H, indol.), 8.25 (d, 2H, benz., J = 8.79 Hz).

Preparation of dye doped polymer films

500 mg of PC was dissolved in 20 mL of $CHCl_3$ followed by the addition of aliquots (0.1 wt%) of 10^{-3} M NPEMI-E stock $CHCl_3$ solution. The resulting clear mixture was then casted into clean Teflon petri-dishes and then left for slow solvent evaporation. Dry 70-80 micron thick films were finally obtained.

Apparatus and Methods

NMR spectra were recorded with a Bruker Advance DRX 400 at room temperature at 400 MHz (^{1}H) and were referred to the residual protons of deuterated solvents.

UV-Vis spectra of both NPEMI-E solutions and films were recorded with a Perkin Elmer Lambda 650 at room temperature.

Emission spectra were measured at room temperature by using a Horiba Jobin–Yvon Fluorolog®-3 spectrofluorometer equipped with a 450 W xenon arc lamp, double-grating excitation and single-grating emission monochromators.

The fluorescence quantum yield (ϕ_F) of NPEMI-E in different solvents was calculated with the comparative method of Williams by using quinine sulfate (ϕ_F = 0.54 in 0.1 M H_2SO_4) and fluorescein (ϕ_F = 0.79 in 0.1 M NaOH) standards.[25,26] Accordingly, 3 solutions of increasing concentration for each standard and dye were prepared followed by recording the absorption and emission spectra at the excitation wavelength ($\lambda_{exc.}$) of dye. For both compounds, the value of integrated fluorescence intensity (area relative to the fluorescence band) is plotted as a function of the absorbance at λ_{exc}. The ϕ_F was calculated using the following equation:

$$\Phi_X = \Phi_{ST}\left(\frac{Grad_X}{Grad_{ST}}\right)\left(\frac{n^2}{n_{ST}^2}\right)$$

Where the subscripts ST and X are the standard and the chromophore respectively, Grad is the gradient from the integrated fluorescence intensity *vs* absorbance and *n* is the refractive index of the solvent (Table 1).

For NPEMI-E/PC films, measurements were performed in dark using F-3000 optic fibre mount apparatus coupled with optic fibre bundles. Light generated from the excitation spectrometer is directly focused on the sample using the optical fibre bundle. Emission from the sample is then directed back through the bundle into the collection port of the sample compartment.[13,14,27] The emission response of the films was tested by exposing the sample held by a steel tripod in a 50 mL beaker closed by a pierced aluminium foil lid (Fig. 2), to 20 mL of various organic solvents of different vapor pressure and PC solubility parameter Δδ (Table 1), at 25 °C and atmospheric pressure.

<Figure 2 near here>

Hue-based quantification of vapochromism

The fluorescence color changes of NPEMI-E/PC films upon exposure to $CHCl_3$ were investigated by means of the hue method described[28] and recently proposed[29,30] as a cost-effective tool to monitor variations in the absorption or emission wavelengths of colorimetric sensors. The hue method consists in converting RGB pictures of the fluorescent samples taken under UV irradiation (using a cheap conventional camera of any kind) to HSV stacks. HSV (Hue,

Saturation and Value) is a color format where the color of each pixel is identified by the coordinates of its position in a cylindrical space.[31] The three different coordinates H, S and V can be determined as follows: H is the color tone expressed as an angular value from 0° to 360°, that corresponds to the wavelength where the emitted light shows its maximum; S locates the point along the cylinder radius, accounting for color purity; V is given by the maximum intensity of the signal produced by the pixel, locating the pixel itself along the cylinder axis. RGB images collected with any digital device can be easily converted in the relevant HSV stack by simple mathematical calculation; images can then be compared in terms of color hue H without artefacts due to different illumination conditions, which would affect only the V and S parameters.[28] Notably, the H, S and V parameters are intrinsically connected with the properties of the emitted light. Considering the light spectrum, H reflects the emission wavelength, S the bandwidth of the peak and V its height. Accordingly, hue values can be used to follow changes in the emission wavelength of a sample, without the need for optical discriminators such as filters or monochromators.

According to this technique, samples of NPEMI-E/PC films exposed to $CHCl_3$ vapors for different time spans were imaged using a Windows Nokia Lumia 625 Smartphone (main camera pixel resolution: 5.0 MP, f-number/aperture: f/2.4, camera focal length: 28 mm). Pictures were imported in open access software ImageJ (National Institute of Health, Bethesda, MD, USA; available for download at https://imagej.nih.gov/ij/), whose built-in plugin was used to transpose them to the HSV color space, thus obtaining a stack of three images (H, S and V) for each picture. Average H values were obtained from selected areas of the H image and rescaled to span the 0-360° range. The S and V layers were used to evaluate the homogeneity of the pictures and to select the region of interest.

Quantum mechanical calculations

Quantum mechanical (QM) calculations of optical absorptions and emission transitions were performed using hybrid DFT functionals (here, B3LYP) and their long-range corrected extensions (here, CAM-B3LYP), which are generally considered suitable for describing molecular systems displaying extended electronic delocalization and their corresponding electronic excitations.[32–35] Solvent effects have been included implicitly by the polarisable continuum model (PCM).[36,37] All QM calculations were performed using the Gaussian09 software package.[38]

RESULTS AND DISCUSSION

Spectroscopic characterization of NPEMI-E in solution

NPEMI-E is well soluble in all solvents characterized by both polar (protic or aprotic) and non-polar nature. The effect of polarity on optical absorption was confirmed by change in color of dilute solutions (10^{-5} M) from pale yellow to intense orange under visible light (Fig. 3a), thus indicating a striking solvatochromism of the dye. Accordingly, under UV lamp ($\lambda_{exc.}$=366 nm), fluorescence changed from blue (*n*-heptane) to red ($CHCl_3$) (Fig. 3b), and it quenched in highly polar solvents including methanol.

<Figure 3 near here>

Absorption and emission spectra of NPEMI-E in different solvents at 10^{-5} M concentration were

recorded. The absorption spectra in solution display three bands (Fig. 4a); while the first two bands were observed at about 230 nm and 280 nm corresponding to n-σ* and n-π* transitions respectively, the third band, issuing from the π-π* transition, splits into three different peaks at 400 nm, 415 nm and 435 nm only in the case of *n*-heptane as solvent. A possible explanation of such behavior could be addressed to the interaction extent between dye and solvent that highlights the vibronic nature of the electronic transitions.[39] A bathochromic shift is noted in absorption spectra as polarity increases from n-hexane (0.1) to DMSO (7.2), which depends on π-π* transition as n-σ* transition bands are not affected by the polarity. On the other hand, a slight hypsochromic shift in methanol is related to specific interactions between the dye and the solvent owing to the hydrogen bonding capability of the latter. Accordingly, upon π-π* excitation, the electron density on heteroatom (i.e., N) decreases as the hydrogen bonding increases resulting in a hypsochromic shift: stronger the hydrogen bonding, more pronounced the shift.[39] The emission spectra in different solvents (Fig. 4b) also highlighted the solvatochromic nature of NPEMI-E with a bathochromic shift of 7008 cm^{-1} in $CHCl_3$ and only 3562 cm^{-1} in *n*-heptane (Table 2). Notably, solvents with the highest polarity index (MeOH and DMSO) completely quenched the emission of NPEMI-E in solution.

<Figure 4 near here>

The Stokes shifts (in wave number) are plotted against solvent orientation polarizability (Δf), i.e. a parameter described in the Lippert–Mataga equation $\Delta f = (J-1)/(2J+1)-(n^2-1)/(2n^2+1)$, where J is the dielectric constant and n is the refractive index of the solvent.[40–42] A variation in Stokes shift as a function of orientation polarizability (Δf) further confirmed the solvatochromic behavior of NPEMI-E in different solvents (Fig. S3). The deviations from linearity in some solvents is ascribed to contributions from specific interactions including intermolecular hydrogen bonding, acid-base interactions, and charge-transfer interactions which are ignored by Lippert-Mataga equation.[43–45]

Table 2. Optical characterization of NPEMI-E in solvents of different polarity.

ϕ_F for NPEMI-E in different solvents was calculated with the comparative method of Williams by using quinine sulphate and fluorescein standards. Notably, ϕ_F decreases in more polar solvents (Table 2). Such a photophysical effect is related to the fact that ICT states are mostly relaxed by non-radiative process resulting in lower fluorescence in polar solvents.[46]

Intramolecular charge transfer (ICT) mechanism

The photophysical nature of NPEMI-E was also effectively investigated by means of QM calculations. Notably, the potential energy surfaces (PESs) of NPEMI-E as a function of the dihedral angle around its double bond (θ), as issuing from both ground and first excited state, were evaluated in $CHCl_3$ (Supporting information, Fig. S1). PESs showed very similar parabola-like profiles centered in correspondence to the planar geometry. These results supported the view of a rather rigid character of the NPEMI-E structure, thus also suggesting the negligible effect of solvent viscosity on the optical features. In contrast, NPEMI-E undergoes a significant change in dipole moment (μ) going from the ground state

to the first excited state, in accordance to an intramolecular charge transfer (ICT). QM calculations of the dipole moment of NPEMI-E in $CHCl_3$, as computed at ground and excited-state equilibrium geometries, provided a value of μ_g = 11.2 Debye and μ_e = 25.6 Debye, respectively. In toluene, μ_e (22.8 Debye) was also higher than μ_g (10.5 Debye), though the dipole moment change was somewhat smaller. Such a strong electronic rearrangement was also supported by the molecular orbitals involved in the first optical transition (Supporting information, Fig. S2), which suggested a partial shift of the electronic density from the indole moiety versus the nitro-phenyl group upon excitation. Note that, despite the appearance of a node in the lowest unoccupied molecular orbital (LUMO) in correspondence of the dye's double bond, the latter did not acquire a pure single-bond character in the excited state, as previously proved by its PES. In turn, this also suggested a relevant role played by the ICT mechanism in NPEMI-E photophysics, in contrast with typical FMRs which undergo significant geometrical rearrangement, is accompanied by ICT. The increase in dipole moment change in $CHCl_3$ with respect to toluene strongly supported the observed bathochromic shift of NPEMI-E emission with solvent polarity, as a result of dipolar solvent relaxation.[39] In a nutshell, solvent reorganization around the chromophore stabilizes more its excited state than the ground state, thus leading to smaller optical transition energies upon emission and, as a consequence, red-shifted fluorescence spectra when going towards more polar solvents. QM calculations of both excitation and emission transition energies of NPEMI-E showed a notable red-shift while going from toluene to $CHCl_3$ (Table 2), in qualitative agreement with experiments. Besides, the computed Stokes' shift consistently increased with solvent polarity, thus further supporting the primary role of the ICT mechanism. Note that deviations between theory and experiments are likely due to intrinsic approximations of the QM model and to the neglected vibronic effects, though the agreement is overall satisfactory and similar to previous computational studies on other molecular probes.[47]

Spectroscopic characterization of NPEMI-E/polymer films

In order to explore the optical properties of NPEMI-E for VOCs sensing, a very small concentration (0.1 wt%) of fluorophore was mixed in PC and films were obtained by solvent casting. Low concentrations of dye were preferred to avoid the effects of aggregation, self-quenching, and self-absorption of chromophore. All PC/NPEMI-E films appeared highly homogeneous and with a thickness of 70-80 μm.

The optical features of NPEMI-E/PC films revealed a Stokes shift of 120 nm (4870 cm^{-1}) (Fig. S4) and a greenish yellow upon excitation at 366 nm (Fig. S4, inset), thus reflecting the behavior of toluene solution (Table 2) being polarity indices comparable (i.e., 2.4 for toluene and 2.9 for PC). This behavior is in accordance with the effect of the polymer matrix on the optical properties of the fluorescent dyes, and suggests a possible and significative influence of vapors of volatile compounds with different polarity.[48,49]

Effect of VOC exposure on the emission spectra of NPEMI-E/Polymer films

Aimed at investigating the vapochromism of NPEMI-E in a much broader way, six solvents of different polarity and with different solvent-polymer interaction were used including *n*-hexane, toluene, diethyl ether, THF, chloroform and methanol. The interaction of different VOCs with PC can be explained on the basis of solubility parameter difference (δ) between PC and solvent ($\Delta\delta=\delta_{PC}-\delta_{solvent}$), since, the Flory-Huggins interaction parameter of some solvents for PC is not available (Table 1). For a better polymer-solvent interaction, the value of δ for both polymer and solvent has to be similar. Fluorescence spectra of NPEMI-E/PC film on exposure to the *n*-hexane are reported in Fig. 5a. Notably, no change in the emission features occurred even after exposing the film up to 35 minutes. A graph of the variation of emission wavelength as a function of the exposure time was also reported and resulted in a constant straight line (Fig. 5a, inset). This result was addressed to the Δδ value of 2.5 $(\text{cal cm}^{-3})^{1/2}$ (Table 1), which evidences a feeble interaction between the polymer matrix and the solvent. This result was also confirmed by using a VOC with higher polarity index but similar solubility parameter difference such as diethyl ether (polarity index = 2.8; Δδ = 2.18 $(\text{cal cm}^{-3})^{1/2}$) Accordingly, on exposure to diethyl ether vapors, the emission spectra did not experience any variation in wavelength (Fig. 5b) being negligible the interaction with the PC matrix.

We further investigated the effect of toluene vapors on the vapochromic response of NPEMI-E/PC films. Notably, toluene is characterized by a similar polarity index (2.4) but a more favorable Δδ with respect to diethyl ether (0.9 $(\text{cal cm}^{-3})^{1/2}$). Notwithstanding the appropriate Δδ, the emission resulted unaffected by solvent exposure, even after 35 min (Fig 5c). This was explained considering the similar polarity between the solvent and the PC matrix. As soon as the solvent molecules get (easily) in contact with the dispersed NPEMI-E, the fluorophore environment does not change in polarity, thus letting the fluorophore maintain the optical features unaltered.

<Figure 5 near here>

By contrast, a clear vapochromism was observed by exposing NPEMI-E/PC film to THF vapors (Fig. 6), i.e. a solvent that shows a good combination of low Δδ (i.e., 0.7 $(\text{cal cm}^{-3})^{1/2}$) and polarity index (4.0). The THF molecules were able to diffuse into the PC matrix and to completely solvate the NPEMI-E molecules, thus promoting a shift in wavelength of 27 nm (from 543 to 570 nm) within 800 seconds (less than 13-14 min, with a time constant of 10^{-3} s^{-1}) of exposure. After that time, the emission wavelength remained mostly unchanged and a plateau was reached (Fig. 6, inset).

<Figure 6 near here>

It is worth noting that the use of $CHCl_3$ as VOC produced an even more pronounced vapochromic response. $CHCl_3$ is characterized by a higher polarity index and a more favorable Δδ (i.e., 4.1 and 0.5 $(\text{cal cm}^{-3})^{1/2}$, respectively than THF. Notably, the strong solvent-polymer interaction fostered NPEMI-E solvation by the absorbed $CHCl_3$ vapors, which in turn caused a pronounced red-shift of the PC film emission wavelength of about 60 nm after a time interval of about 10 min only (Fig. 7). Moreover, the emission wavelength variation of the maximum as a function of $CHCl_3$ vapors exposure time further supports the evident solvatochromism (Fig. 7 inset). Data were fitted with good correlation using the mono-exponential growth function. Since the fitting procedure was not completely accurate in the initial part of the

experiment we omitted to convert it into linear relationship. The time constant was about 4 times higher than that calculated for THF as VOC (i.e., $4 \cdot 10^{-3}$ s^{-1} against 10^{-3} s^{-1}), also promoted by the greater vapor pressure of $CHCl_3$ with respect that of the latter (i.e., 158.4 mm Hg against 142 mm Hg).

<Figure 7 near here>

The pronounced wavelength shift of about 60 nm produced a clear variation of the emission color of the films from green to yellow and eventually to a dark yellow after a long time of exposure (about 30 min), which can be easily detected by the naked eye even during the first min of the experiments.

We finally tested the influence of MeOH vapors on the vapochromic behavior of NPEMI-E/PC films. MeOH is a very polar solvent with the highest polarity index of 5.1 but with an adverse $\Delta\delta$ of -5 $(cal\ cm^{-3})^{1/2}$. Nevertheless, notwithstanding the highest $\Delta\delta$ for methanol and the lower vapor pressure compared to diethyl ether for example, NPEMI-E/PC films experienced a 10 nm shift in their emission wavelength (Fig. 8).

<Figure 8 near here>

This phenomenon could be possibly addressed to the vapor molecules that get in contact with the PC surface where some NPEMI-E molecules could be distributed during the solvent evaporation.[50,51] Differently from dye molecules molecularly dissolved within the PC bulk, those at the surface can be promptly solvated by the incoming solvent, thus providing the shift in wavelength. Even if the high polarity index of MeOH should suggest a more pronounced wavelength shift, the solvatochromic effect is only partial since only fluorophore molecules at the film surfaces were affected by VOC solvation.

The remaining NPEMI-E molecules were not involved in the phenomenon being dispersed in the unaffected PC bulk. Overall, on the account of the reported experiments, NPEMI-E/PC films revealed the strongest vapochromic feature towards $CHCl_3$ vapors.

Reproducibility and reversibility of the behavior of NPEMI-E/PC films

In order to explore the reproducibility and reversibility of the vapochromic response, the NPEMI-E/PC films exposed to $CHCl_3$ vapors were dried at 50 °C for 5 min in a ventilated stove to remove residual solvent from the film. This procedure was repeated after every exposure. The reproducibility depends on the NPEMI-E emission response while the reversibility feature is associated to the PC matrix, including the changes in polymer structure due to solvent interaction. Fig. 9 shows that NPEMI-E/PC films exhibited excellent reversibility and good reproducibility to successive cycles of $CHCl_3$ vapors exposure. We speculated that the faster wavelength variation for the successive exposure cycles could be possibly addressed to a partial segregation of fluorophore at the surface induced during film dryness. The solvated NPEMI-E molecules were therefore forced to move closer to the film surface, thus rendering the successive vapochromism more prompt to occur.

<Figure 9 near here>

HUE-based quantification of $CHCl_3$ exposure

NPEMI-E/PC samples exposed to $CHCl_3$ for different spans of time were imaged and the RGB pictures were converted to the HSV (Hue, Saturation and Value) color space. Average H

values were obtained from selected areas of the H image and rescaled to span the 0-360° range. The S and V layers were used to evaluate the homogeneity of the pictures and to select the region of interest. Average H values showed a decrease with exposure time, reaching a plateau after about 10 min of exposure to solvent (Fig. 10a).

<Figure 10 near here>

It is worth noting that this behavior is in good agreement with the spectroscopic data shown in Fig. 7 and also accounts for the fluorescence color variation that can be observed in Fig. 10b. The hue parameter allowed therefore for the effective extraction of spectral information from digital color images of NPEMI-E/PC samples. This very simple and inexpensive method permitted to follow changes in the sample emission upon exposure to $CHCl_3$ without the need for wavelength discriminators.

CONCLUSIONS

We have demonstrated that a solvatochromic fluorophore, namely NPEMI-E, when dispersed in films of PC experiences a selective and pronounced response towards polar and PC interacting VOCs such as chloroform. NPEMI-E showed excellent solubility in many classes of solvents with a change in color, depending on solvent polarity. The experimental and computed Stokes' shift that consistently increased with solvent polarity supported the primary role of the ICT mechanism in the photophysics of the dye. When embedded in PC films at very low content (0.1 wt%), NPEMI-E exhibited strong fluorescence variations visible to the naked eye upon exposure to saturated atmospheres of polar and well-interacting VOCs only. VOCs with an unfavorable solubility parameter difference (Δδ) or polarity index (n-hexane, toluene and MeOH), were not active in promoting an effective vapochromic response. By contrast, a remarkable, fast and reversible vapochromic response was registered for chloroform vapors, and the phenomenon was effectively quantified by hue determination as well. This simple and low-cost approach can then be envisioned to exploit NPEMI-E/PC films as vapochromic films in the production of inexpensive chloroform optical sensors.

ACKNOWLEDGEMENTS

Dr. Francesco Greco and Prof. Arturo Colligiani are kindly acknowledged for the preparation of NPEMI-E.

REFERENCES:

1 L. B. Desmonts, D. N. Reinhoudt and M. Crego-Calama, *Chem. Soc. Rev.*, **2007**, 36, 993–1017.

2 S. Raut, J. Kimball, R. Fudala, H. Doan, B. Maliwal, N. Sabnis, A. Lacko, I. Gryczynski, S. V Dzyuba and Z. Gryczynski, *Phys. Chem. Chem. Phys.*, **2014**, 16, 27037–42.

3 A. S. Klymchenko, *Acc. Chem. Res.*, **2017**, DOI: 10.1021/acs.accounts.6b00517.

4 B. Liu and B. Z. Tang, *Macromol. Rapid Commun.*, **2013**, 34, 704.

5 J. Mei, N. L. C. Leung, R. T. K. Kwok, J. W. Y. Lam and B. Z. Tang, *Chem. Rev.*, **2015**, 115, 11718–11940.

6 A. P. Silva, H. Q. N. Gunaratne, T. Gunnlaugsson, A. J. M. Huxley, C. P. McCoy, J. T. Rademacher and T. E. Rice, *Chem. Rev.*, **1997**, 97, 1515–1566.

7 J. Mei, Y. Hong, J. W. Y. Lam, A. Qin, Y. Tang and B. Z. Tang, *Adv. Mater.*, **2014**, 26, 5429–5479.

8 F. Ciardelli, G. Ruggeri and A. Pucci, *Chem. Soc. Rev.*, **2013**, 42, 857–70.

9 M. A. Haidekker and E. A. Theodorakis, *J. Biol. Eng.*, **2010**, 4, 11.

10 M.A. Haidekker, N. Matthew, M. Adnan, L. Darcy, D. Marianna, in *Advanced Fluorescence Reporters in Chemistry and Biology I: Fundamentals and Molecular Design*, ed. Demchenko A.P, Springer-Verlag, Berlin Heidelberg, **2010**, pp. 267–308.

11 M. A. Haidekker and E. A. Theodorakis, *Org. Biomol. Chem.*, **2007**, 5, 1669–78.

12 M. A. Haidekker, T. P. Brady, D. Lichlyter and E. A. Theodorakis, *J. Am. Chem. Soc.*, **2006**, 128, 398–399.

13 P. Minei, M. Koenig, A. Battisti, M. Ahmad, V. Barone, T. Torres, D. M. Guldi, G. Brancato, G. Bottari and A. Pucci, *J. Mater. Chem. C*, **2014**, 2, 9224–9232.

14 P. Minei, M. Ahmad, V. Barone, G. Brancato, E. Passaglia, G. Bottari and A. Pucci, *Polym. Adv. Technol.*, **2016**, 27, 429–435.

15 P. Minei and A. Pucci, *Polym. Int.*, **2016**, 65, 609–620.

16 G. Martini, E. Martinelli, G. Ruggeri, G. Galli and A. Pucci, *Dye. Pigment.*, **2015**, 113, 47–54.

17 G. Iasilli, F. Martini, P. Minei, G. Ruggeri and A. Pucci, *Faraday Discuss.*, **2016**, 196, 113–129.

18 M. C. Janzen, J. B. Ponder, D. P. Bailey, C. K. Ingison and K. S. Suslick, *Anal. Chem.*, **2006**, 78, 3591–3600.

19 B. Huang, C. Lei, C. Wei and G. Zeng, *Environ. Int.*, **2014**, 71, 118–138.

20 R. Angelone, F. Ciardelli, A. Colligiani, F. Greco, P. Masi, A. Romano, G. Ruggeri and J. L. Stehlé, in *IOP Conference Series: Materials Science and Engineering*, Strasbourg, France, **2009**.

21 R. Angelone, F. Ciardelli, A. Colligiani, F. Greco, P. Masi, A. Romano, G. Ruggeri and J.-L. Stehlé, *Appl. Opt.*, **2008**, 47, 6680–6691.

22 D.R.Lide , *Handbook of Chemistry and Physics*, CRC Press, Boca Raton, FL, **1978**.

23 J. Brandrup, E. Immergut and E. A. Grulke, *Polymer handbook*, John Wiley & Sons, Inc., New York, **1990**.

24 A. A. Colligiani, F. Brustolin, V. Castelvetro, F. Ciardelli and G. Ruggeri, in *Proc. SPIE 4104, Organic Photorefractives, Photoreceptors, and Nanocomposites*, San Diego, CA, USA, **2000**.

25 A. T. R. Williams, S. A. Winfield and J. N. Miller, *Analyst*, **1983**, 108, 1067–1071.

26 H. J. Yvon, *A guide to recording Fluorescence Quantum Yields*, Horiba Jobin Yvon, **2012**.

27 I. Platonova, A. Branchi, M. Lessi, G. Ruggeri, F. Bellina and A. Pucci, *Dye. Pigment.*, **2014**, 110, 249–255.

28 K. Cantrell, M. M. Erenas, I. De Orbe-Payá and L. F. Capitán-Vallvey, *Anal. Chem.*, **2010**, 82, 531–542.

29 A. Hakonen, J. E. Beves and N. Strömberg, *Analyst*, **2014**, 139, 3524–7.

30 A. Battisti, P. Minei, A.Pucci, and R.

Bizzarri, *Chem. Commun.*, **2016,** 53, 248–251.

31 A. R. Smith, *ACM SIGGRAPH Comput. Graph.*, **1978**, 12, 12–19.

32 F. J. Devlin, J. W. Finley, P. J. Stephens and M. J. Frisch, *J. Phys. Chem.*, **1995**, 99, 16883–16902.

33 D. Jacquemin, E. A. Perpete, I. Ciofini and C. Adamo, *Acc. Chem. Res.*, **2009**, 42, 326–334.

34 T. Yanai, D. P. Tew and N. C. Handy, *Chem. Phys. Lett.*, **2004**, 393, 51–57.

35 G. Brancato, G. Signore, P. Neyroz, D. Polli, G. Cerullo, G. Abbandonato, L. Nucara, V. Barone, F. Beltram and R. Bizzarri, *J. Phys. Chem. B*, **2015**, 119, 6144–6154.

36 V. Barone and M. Cossi, *J. Phys. Chem. A*, **1998**, 102, 1995–2001.

37 M. Cossi, N. Rega, G. Scalmani and V. Barone, *J. Comput. Chem.*, **2003**, 24, 669–681.

38 G. M. J. Frisch, W. Trucks and E. Schlegel, *Gaussian 09, Revision A. 1; Gaussian*, Wallingford CT, **2009**.

39 B. Valeur and M. N. Berberan-Santos, *Molecular Fluorescence: Principles and Applications*, Wiley-VCH, Weinheim, **2012**.

1 L. B. Desmonts, D. N. Reinhoudt and M. Crego-Calama, *Chem. Soc. Rev.*, **2007**, 36, 993–1017.

2 S. Raut, J. Kimball, R. Fudala, H. Doan, B. Maliwal, N. Sabnis, A. Lacko, I. Gryczynski, S. V Dzyuba and Z. Gryczynski, *Phys. Chem. Chem. Phys.*, **2014**, 16, 27037–42.

3 A. S. Klymchenko, *Acc. Chem. Res.*, **2017**, DOI: 10.1021/acs.accounts.6b00517.

4 B. Liu and B. Z. Tang, *Macromol. Rapid Commun.*, **2013**, 34, 704.

5 J. Mei, N. L. C. Leung, R. T. K. Kwok, J. W. Y. Lam and B. Z. Tang, *Chem. Rev.*, **2015**, 115, 11718–11940.

6 A. P. Silva, H. Q. N. Gunaratne, T. Gunnlaugsson, A. J. M. Huxley, C. P. McCoy, J. T. Rademacher and T. E. Rice, *Chem. Rev.*, **1997**, 97, 1515–1566.

7 J. Mei, Y. Hong, J. W. Y. Lam, A. Qin, Y. Tang and B. Z. Tang, *Adv. Mater.*, **2014**, 26, 5429–5479.

8 F. Ciardelli, G. Ruggeri and A. Pucci, *Chem. Soc. Rev.*, **2013**, 42, 857–70.

9 M. A. Haidekker and E. A. Theodorakis, *J. Biol. Eng.*, **2010**, 4, 11.

10 M.A. Haidekker, N. Matthew, M. Adnan, L. Darcy, D. Marianna, in *Advanced Fluorescence Reporters in Chemistry and Biology I: Fundamentals and Molecular Design*, ed. Demchenko A.P, Springer-Verlag, Berlin Heidelberg, **2010**, pp. 267–308.

11 M. A. Haidekker and E. A. Theodorakis, *Org. Biomol. Chem.*, **2007**, 5, 1669–78.

12 M. A. Haidekker, T. P. Brady, D. Lichlyter and E. A. Theodorakis, *J. Am. Chem. Soc.*, **2006**, 128, 398–399.

13 P. Minei, M. Koenig, A. Battisti, M. Ahmad, V. Barone, T. Torres, D. M. Guldi, G. Brancato, G. Bottari and A. Pucci, *J. Mater. Chem. C*, **2014**, 2, 9224–9232.

14 P. Minei, M. Ahmad, V. Barone, G. Brancato, E. Passaglia, G. Bottari and A. Pucci, *Polym. Adv. Technol.*, **2016**, 27, 429–435.

15 P. Minei and A. Pucci, *Polym. Int.*, **2016**, 65, 609–620.

16 G. Martini, E. Martinelli, G. Ruggeri, G.

Galli and A. Pucci, *Dye. Pigment.*, **2015**, 113, 47–54.

17 G. Iasilli, F. Martini, P. Minei, G. Ruggeri and A. Pucci, *Faraday Discuss.*, **2017**, 196, 113–129.

18 M. C. Janzen, J. B. Ponder, D. P. Bailey, C. K. Ingison and K. S. Suslick, *Anal. Chem.*, **2006**, 78, 3591–3600.

19 B. Huang, C. Lei, C. Wei and G. Zeng, *Environ. Int.*, **2014**, 71, 118–138.

20 R. Angelone, F. Ciardelli, A. Colligiani, F. Greco, P. Masi, A. Romano, G. Ruggeri and J. L. Stehlé, in *IOP Conference Series: Materials Science and Engineering*, Strasbourg, France, **2009**.

21 R. Angelone, F. Ciardelli, A. Colligiani, F. Greco, P. Masi, A. Romano, G. Ruggeri and J.-L. Stehlé, *Appl. Opt.*, **2008**, 47, 6680–6691.

22 D.R.Lide , *Handbook of Chemistry and Physics*, CRC Press, Boca Raton, FL, **1978**.

23 J. Brandrup, E. Immergut and E. A. Grulke, *Polymer handbook*, John Wiley & Sons, Inc., New York, **1990**.

24 A. A. Colligiani, F. Brustolin, V. Castelvetro, F. Ciardelli and G. Ruggeri, in *Proc. SPIE 4104, Organic Photorefractives, Photoreceptors, and Nanocomposites*, San Diego, CA, USA, **2000**.

25 A. T. R. Williams, S. A. Winfield and J. N. Miller, *Analyst*, **1983**, 108, 1067–1071.

26 H. J. Yvon, *A guide to recording Fluorescence Quantum Yields*, Horiba Jobin Yvon, **2012**.

27 I. Platonova, A. Branchi, M. Lessi, G. Ruggeri, F. Bellina and A. Pucci, *Dye. Pigment.*, **2014**, 110, 249–255.

28 K. Cantrell, M. M. Erenas, I. De Orbe-Payá and L. F. Capitán-Vallvey, *Anal. Chem.*, **2010**, 82, 531–542.

29 A. Hakonen, J. E. Beves and N. Strömberg, *Analyst*, **2014**, 139, 3524–7.

30 A. Battisti, P. Minei, A.Pucci, and R. Bizzarri, *Chem. Commun.*, **2016,** 53, 248–251.

31 A. R. Smith, *ACM SIGGRAPH Comput. Graph.*, **1978**, 12, 12–19.

32 F. J. Devlin, J. W. Finley, P. J. Stephens and M. J. Frisch, *J. Phys. Chem.*, **1995**, 99, 16883–16902.

33 D. Jacquemin, E. A. Perpete, I. Ciofini and C. Adamo, *Acc. Chem. Res.*, **2009**, 42, 326–334.

34 T. Yanai, D. P. Tew and N. C. Handy, *Chem. Phys. Lett.*, **2004**, 393, 51–57.

35 G. Brancato, G. Signore, P. Neyroz, D. Polli, G. Cerullo, G. Abbandonato, L. Nucara, V. Barone, F. Beltram and R. Bizzarri, *J. Phys. Chem. B*, **2015**, 119, 6144–6154.

36 V. Barone and M. Cossi, *J. Phys. Chem. A*, **1998**, 102, 1995–2001.

37 M. Cossi, N. Rega, G. Scalmani and V. Barone, *J. Comput. Chem.*, **2003**, 24, 669–681.

38 G. M. J. Frisch, W. Trucks and E. Schlegel, *Gaussian 09, Revision A. 1; Gaussian*, Wallingford CT, **2009**.

39 B. Valeur and M. N. Berberan-Santos, *Molecular Fluorescence: Principles and Applications*, Wiley-VCH, Weinheim, **2012**.

40 B. Mysliwa-Kurdziel, K. Solymosi, J. Kruk, B. Boddi and K. Strzalka, *Eur. Biophys. J.*, **2008**, 37, 1185–1193.

41 H. Singh, J. Sindhu and J. M. Khurana,

Sensors Actuators, B Chem., **2014**, 192, 536–542.

42 A. E. Da Hora Machado, J. A. De Miranda, S. Guilardi, D. E. Nicodem and D. Severino, *Spectrochim. Acta - Part A Mol. Biomol. Spectrosc.*, **2003**, 59, 345–355.

43 A. Matwijczuk, D. Kluczyk, A. Gorecki, A. Niewiadomy and M. Gagos, *J. Phys. Chem. B*, **2016**, 120, 7958–7969.

44 Z. Diwu, Y. Lu, C. Zhang, D. H. Klaubert and R. P. Haugland, *Photochem. Photobiol.*, **1997**, 66, 424–431.

45 R. W. Sinkeldam and Y. Tor, *Org. Biomol. Chem.*, **2007**, 5, 2523–2528.

46 A. Hawe, M. Sutter and W. Jiskoot, *Pharm. Res.*, **2008**, **25**, 1487–1499.

47 M. Koenig, G. Bottari, G. Brancato, V. Barone, D. M. Guldi and T. Torres, *Chem. Sci.*, **2013**, 4, 2502.

48 C. Reichardt, *Solvents and Solvent Effects in Organic Chemistry*, Wiley-VCH Verlag GmbH & Co., KGaA, Weinheim, **2011**.

49 C. Reichardt, *Pure Appl. Chem.*, **2008**, 80, 1415–1432.

50 N. Tirelli, S. Amabile, C. Cellai, A. Pucci, L. Regoli, G. Ruggeri and F. Ciardelli, *Macromolecules*, **2001**, 34, 2129–2137.

51 A. Pucci, N. Tirelli, G. Ruggeri and F. Ciardelli, *Macromol. Chem. Phys.*, **2005**, 206, 102–111.

Table 1. Vapor pressure, polarity[22], solubility parameter difference Δδ (PC)[23] and refractive index[22] of the utilized solvents.

Solvent	Vapor pressure (mmHg)	Polarity index	Δδ $(cal\ cm^{-3})^{1/2}$	Refractive index
***n*-hexane**	12.4	0.1	2.5	1.38
Et_2O	440	2.8	2.18	1.35
$CHCl_3$	158.4	4.1	0.5	1.44
Methanol	97.6	5.1	-5	1.32
THF	142	4.0	0.7	1.40
Toluene	28.5	2.4	0.9	1.49

Table 2. Optical characterization of NPEMI-E in solvents of different polarity.

Solvent	Δf	Absorption λ_{max} (nm)	Emission λ_{max} (nm)	Stokes Shift (cm^{-1})	ϕ_F
***n*-heptane**	0.0025	415	487	3562	0.03(a)
Toluene	0.0132	424(385[c])	535(480[c])	4893	0.18 (a)
Et_2O	0.1634	417	538	5393	0.23 (a)
THF	0.2086	432	580	5907	0.14 (b)
$CHCl_3$	0.1469	438(403[c])	632(523[c])	7008	0.02 (b)

(a) Quinine Sulphate (Excitation Wavelength = 380 nm)[25,26]
(b) Fluorescein (Excitation wavelength = 490 nm)[25,26]
(C) Results from QM calculations.

FIGURE 1. Molecular structure of 3-[2-(4-nitrophenyl) ethenyl]-1-(2-ethylhexyl)-2-methylindole (NPEMI-E)

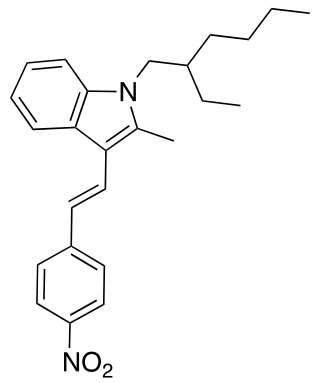

FIGURE 2. Setup used to study the solvatochromism of NPEMI-E/PC films. Reproduced from Ref. 17 with permission from The Royal Society of Chemistry

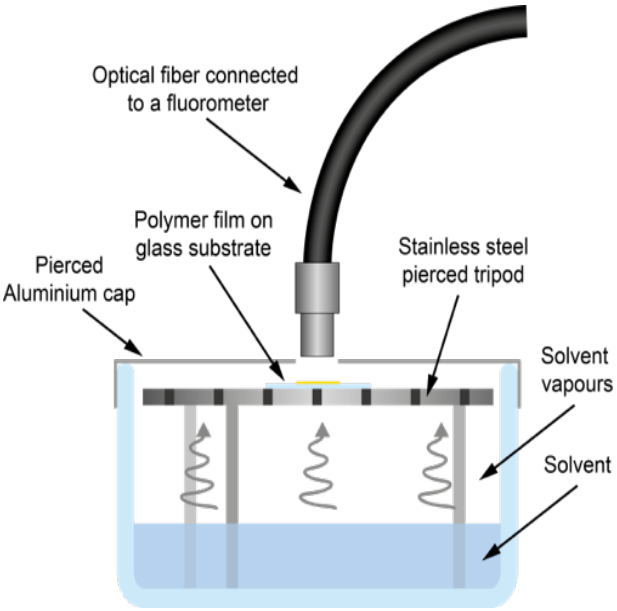

FIGURE 3. From left to right: NPEMI-E solution in *n*-heptane, toluene, diethylether, tetrahyrofuran, chloroform, methanol, (a) under visible light and (b) under the UV lamp illumination at 366 nm.

(a)

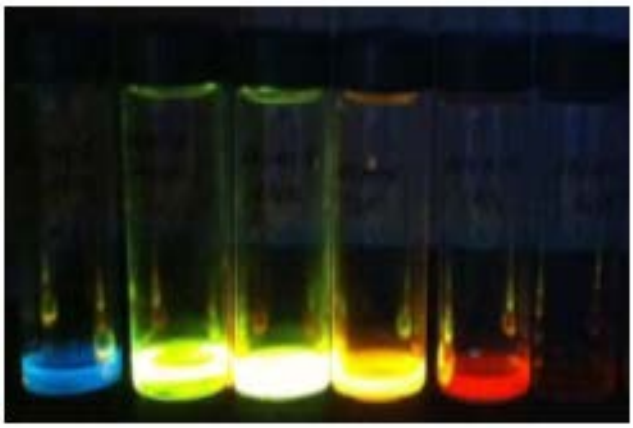

(b)

FIGURE 4. (a) Absorbance spectra (b) and normalized emission spectra ($\lambda_{exc.}$=380nm) of 10^{-5} M NPEMI-E solutions in different solvents. Fluorescence spectra in MeOH and DMSO were omitted due to negligible emission.

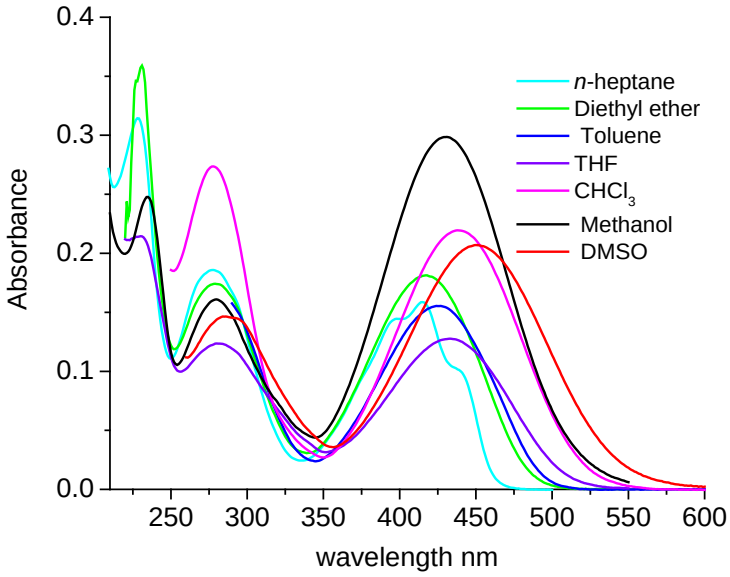

(a)

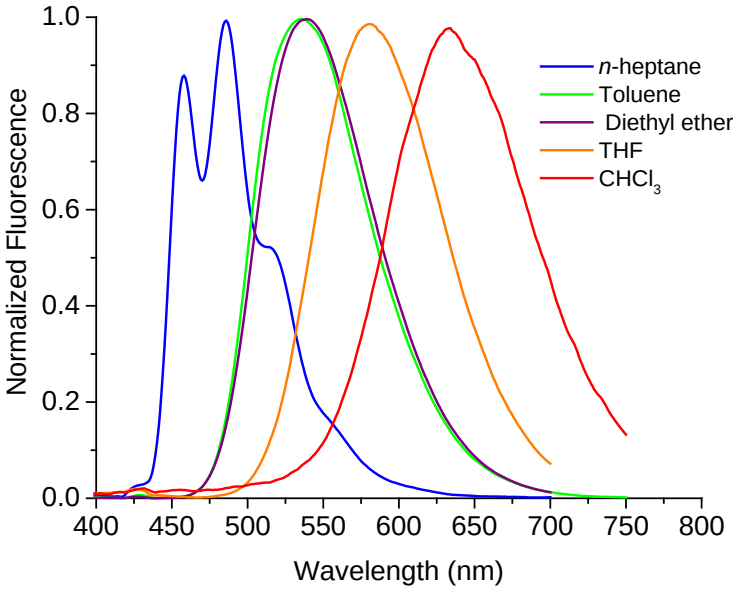

(b)

FIGURE 5. Normalized fluorescence intensity of NPEMI-E/PC exposed to the vapours of (a) *n*-hexane (b) Diethyl ether and (c) Toluene vapours for a time interval of 35 min ($\lambda_{exc.}$=430nm). Variation of maximum emission of PC/NPEMI-E as a function of exposure time to the vapours of n-hexane (Inset a), diethyl ether (inset b), and toluene (inset c).

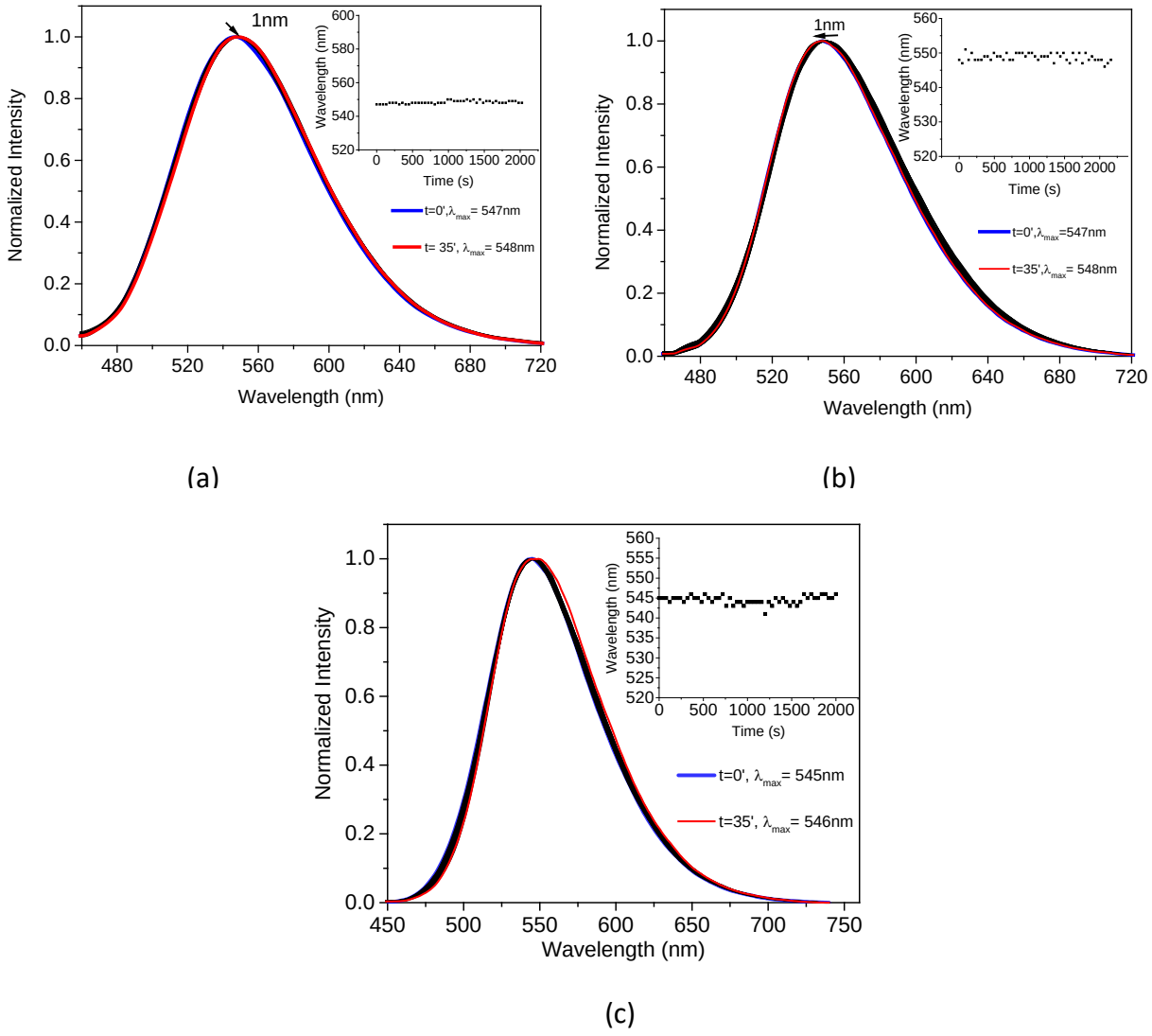

FIGURE 6. Fluorescence of NPEMI-E/PC exposed to THF for a time interval of 35 min ($\lambda_{exc.}$=430nm). Variation of the maximum emission of NPEMI-E/PC film as a function of exposure time to THF (▪). The wavelength shift with time exposure was fitted with mono-exponential ($y = y_0+A\cdot e^{(-x/t)}$) function with 1/t as time constant (solid line, inset).

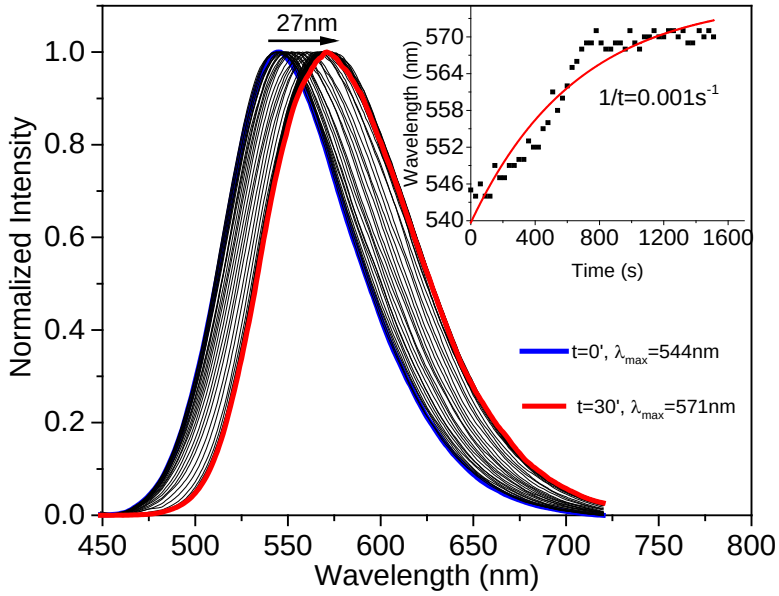

FIGURE 7. Normalized emission of NPEMI-E/PC exposed to $CHCl_3$ for a time interval of 13 min ($\lambda_{exc.}$=430nm). Variation of maximum emission of PC/NPEMI-E film as a function of exposure time to chloroform (▪).The wavelength shift with time exposure was fitted with mono-exponential ($y = y_0+A\cdot e^{(-x/t)}$) function with 1/t as time constant (solid line, inset).

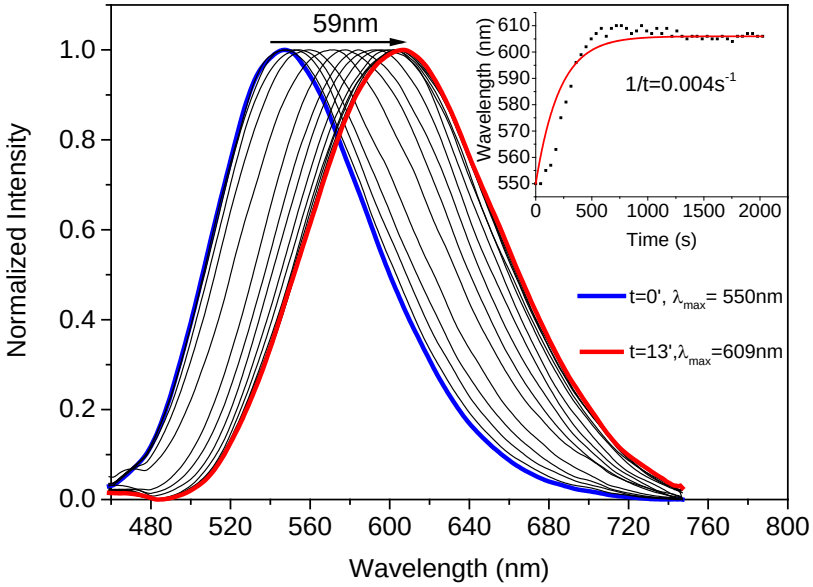

FIGURE 8. Fluorescence of NPEMI-E/PC film exposed to MeOH for a time interval of 35 min ($\lambda_{exc.}$=430nm). Variation of the maximum emission of NPEMI-E/PC film as a function of exposure time to methanol (▪).The wavelength shift with time exposure was fitted with mono-exponential ($y = y_0+A\cdot e^{(-x/t)}$) function with 1/t as time constant (solid line, inset).

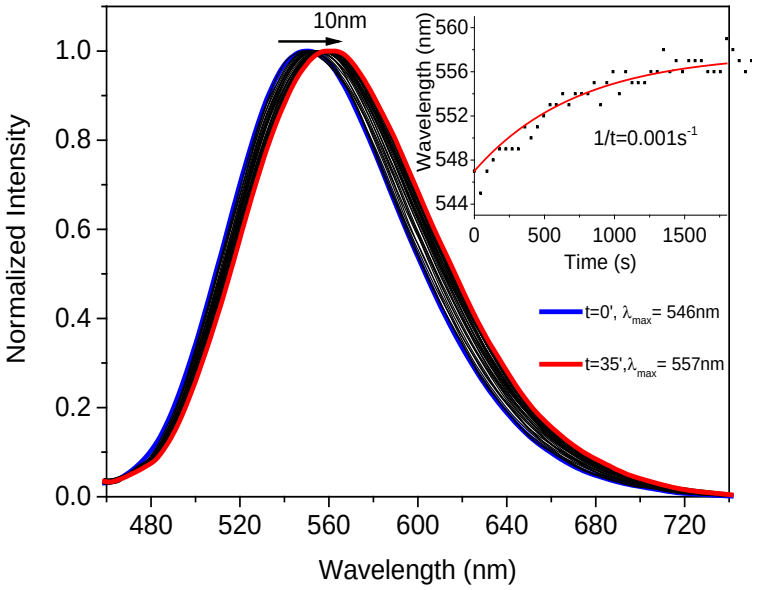

FIGURE 9. Variation of the wavelength at emission maximum of NPEMI-E/PC film on exposure to vapours of $CHCl_3$ for 3 successive cycles. The vertical dashed lines indicate storage time of 5 min at 50°C (λ_0 is the wavelength at emission maximum of the film before vapours exposure).

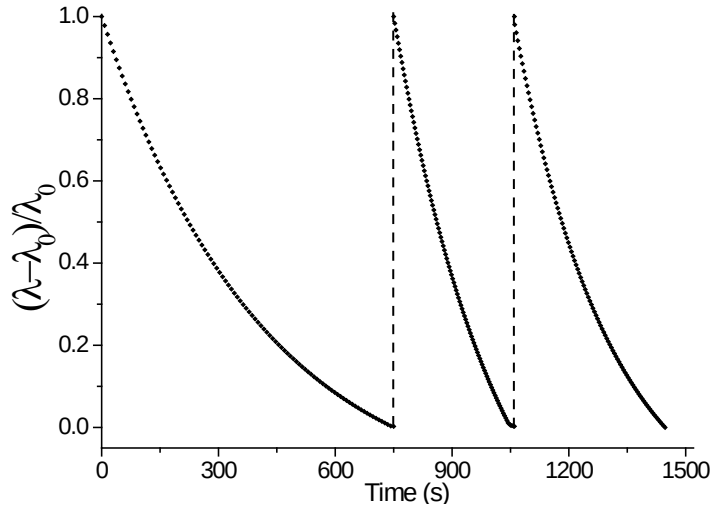

FIGURE 10. (a) Hue values vs $CHCl_3$ exposure time for NPEMI-E/PC films. (b) Images of NPEMI-E/PC samples after different exposure times to $CHCl_3$. Top: original RGB images. Bottom: hue layer after the conversion to HSV. Gray scale bar on the right refers to images in the bottom row only.

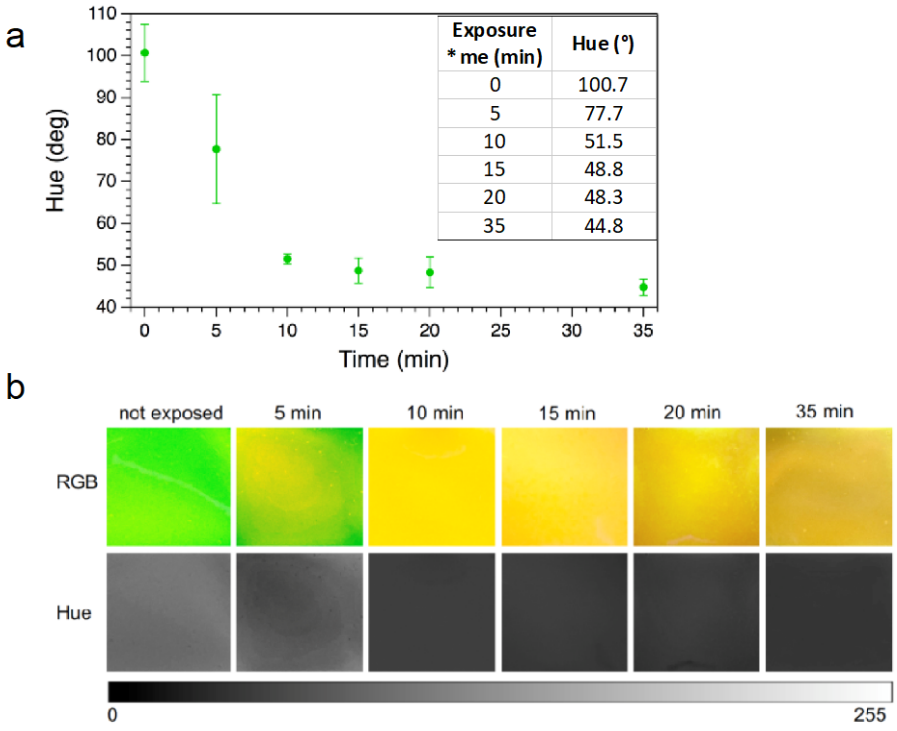

TOC

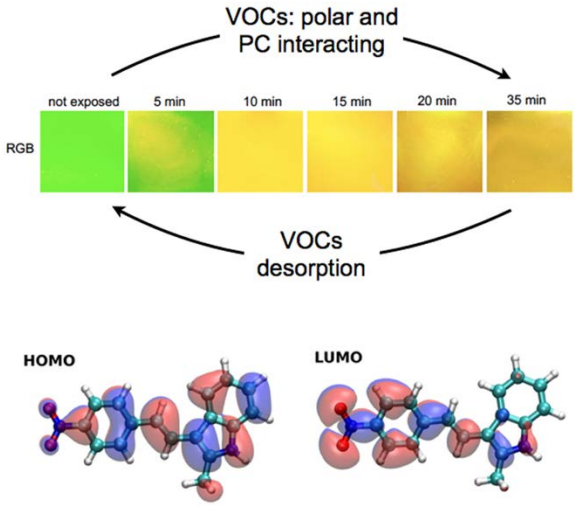

Solvatochromic indole fluorophores characterized by intramolecular charge transfer (ICT) character endow polycarbonate (PC) films with a great vapochromic features once exposed to saturated atmospheres of different volatile organic compounds (VOCs). The thin films show remarkable and reversible vapochromism when exposed to VOCs with high polarity index and favorable interaction with PC matrix such as $CHCl_3$. The vapochromism is also effectively quantified by the very simple and inexpensive hue determination method.